



Published in final edited form as:

Brain Res. 2017 May 15; 1663: 87–94. doi:10.1016/j.brainres.2017.03.009.

Inhibition of Kir4.1 potassium channels by quinacrine

Leticia G. Marmolejo-Murillo¹, Iván A. Aréchiga-Figueroa², Meng Cui³, Eloy G. Moreno-Galindo¹, Ricardo A. Navarro-Polanco¹, José A. Sánchez-Chapula¹, Tania Ferrer¹, and Aldo A. Rodríguez Menchaca⁴

¹Centro Universitario de Investigaciones Biomédicas, Universidad de Colima, Colima, Col 28045, México

²CONACYT, Facultad de Medicina, Universidad Autónoma de San Luis Potosí, San Luis Potosí, SLP 78210, México

³Department of Physiology and Biophysics, Virginia Commonwealth University, School of Medicine, Richmond, Virginia 23298, USA

⁴Departamento de Fisiología y Biofísica, Facultad de Medicina, Universidad Autónoma de San Luis Potosí, SLP 78210, México

Abstract

Inwardly rectifying potassium (Kir) channels are expressed in many cell types and contribute to a wide range of physiological processes. Particularly, Kir4.1 channels are involved in the astroglial spatial potassium buffering. In this work, we examined the effects of the cationic amphiphilic drug quinacrine on Kir4.1 channels heterologously expressed in HEK293 cells, employing the patch clamp technique. Quinacrine inhibited the currents of Kir4.1 channels in a concentration and voltage dependent manner. In inside-out patches, quinacrine inhibited Kir4.1 channels with an IC₅₀ value of $1.8 \pm 0.3 \mu\text{M}$ and with extremely slow blocking and unblocking kinetics. Molecular modeling combined with mutagenesis studies suggested that quinacrine blocks Kir4.1 by plugging the central cavity of the channels, stabilized by the residues E158 and T128. Overall, this study shows that quinacrine blocks Kir4.1 channels, which would be expected to impact the potassium transport in several tissues.

Keywords

Kir4.1 channels; quinacrine; cationic amphiphilic drugs

Corresponding authors: Aldo A. Rodríguez-Menchaca⁴, Av. Venustiano Carranza #2405, Col. Los Filtros, San Luis Potosí, SLP, 78210, México. aldo.rodiguez@uaslp.mx. Tania Ferrer¹, Av. 25 de Julio 965 Col. Villas San Sebastián, C.P. 28045 Colima, Colima, México. tania@ucol.mx.

Publisher's Disclaimer: This is a PDF file of an unedited manuscript that has been accepted for publication. As a service to our customers we are providing this early version of the manuscript. The manuscript will undergo copyediting, typesetting, and review of the resulting proof before it is published in its final citable form. Please note that during the production process errors may be discovered which could affect the content, and all legal disclaimers that apply to the journal pertain.

1. Introduction

The inwardly rectifying potassium (Kir) channels comprise a superfamily composed of seven subfamilies (Kir1-7) containing at least 16 members in mammals. Kir channels play critical roles in the regulation of multiple cellular functions including repolarization of action potentials, K⁺ homeostasis and hormone secretion (Hibino et al., 2010; Swale et al., 2014). Among the Kir family, the Kir4.1 subunit is predominantly expressed in brain astrocytes mediating, at least partly, the astroglial spatial K⁺ buffering (Neusch et al., 2006; Kucheryavik et al., 2007). This process unidirectionally transports excess extracellular K⁺ to the regions of low K⁺ (Simard and Nedergaard, 2004). Additionally, Kir4.1 channels are expressed in the renal epithelia (Lourdel et al., 2002; Lachheb et al., 2008), where they are responsible for the basolateral K⁺ recycling in the distal tubules (Palygin et al., 2016).

The reduced expression or dysfunction of Kir4.1 channels seems to be involved in several diseases (Loudon and Fry, 2014; Nwaobi et al., 2016). Recent studies showed that loss-of-function mutations of the human gene (*KCNJ10*) encoding Kir4.1 channels are responsible for the SeSAME/EAST syndrome, an autosomal recessive disorder characterized by seizures, sensorineural deafness, ataxia, intellectual disability and electrolyte imbalance (Bockenbauer et al., 2009; Scholl et al., 2009; Reichold et al., 2010). Genetic variations of *KCNJ10* have also been related to epilepsy (Buono et al., 2004; Ferraro et al., 2004; Lenzen et al., 2005; Dai et al., 2015), a group of neurological diseases characterized by seizure disorders. Other diseases associated to Kir4.1 channels include spinocerebellar ataxia (Gilliam et al., 2014), autism (Sicca et al., 2011), Alzheimer disease (Wilcock et al., 2009), and Huntington disease (Tong et al., 2014).

Despite Kir4.1 channels appear an essential protein implicated in several key astrocytic and renal functions, pharmacological studies of these channels are limited. The glucocorticoid dexamethasone and the antibiotic minocycline have been shown to increase the expression of Kir4.1 channels (Zhao et al., 2011; Zhang et al., 2011). Dexamethasone increases the expression of Kir4.1 channels by twofold in healthy retina and prevents the loss of these channels in inflamed retina (Zhao et al., 2011), whereas minocycline rescues the levels of Kir4.1 channels in diabetic rat retinas (Zhang et al., 2011). There are also a few studies reporting inhibition of Kir4.1 channels by several drugs (Su et al., 2007; Ohno et al., 2007; Furutani et al., 2009, Rodríguez-Menchaca et al., 2016). It has been speculated that inhibition of Kir4.1 channels by antidepressants may increase the neuronal activity by reducing the astroglial K⁺ buffering, which could be involved in their clinical effects for depression (Ohno et al., 2007). Although targeting Kir4.1 channels may be beneficial in certain conditions as mentioned above, their chronic inhibition could lead to unwanted effects, similar to those observed in patients presenting loss-of-function mutations on Kir4.1 channels. Therefore, a better understanding of the mechanisms of drug actions on Kir4.1 channels will enable the design of safer and effective drugs to treat Kir4.1 related diseases.

In this work, we evaluated the inhibition of Kir4.1 channels by quinacrine, an old antimalarial drug that has gained broad attention in drug-repositioning studies since it has been shown to possess anti-cancer properties (Neznanov et al., 2009; Preet et al., 2012; Khurana et al., 2015; Ericksson et al., 2015; Das et al., 2016). Here, we show that quinacrine

plugs the central cavity of Kir4.1 channels in a voltage-dependent manner and with slow blocking and unblocking kinetics.

2. Results

2.1. Inhibition of Kir4.1 channels by quinacrine

The effect of quinacrine was examined using the whole-cell configuration of the patch clamp technique in HEK293 cells transfected with Kir4.1 cDNA. The cells were held at -35 mV and voltage step-pulses (1 s in duration) were successively applied from -120 mV to $+60$ mV (with 20 mV increments) every 10 s. Each drug concentration was perfused until the steady-state effect was achieved (4–6 min). In control conditions (Fig. 1A and B, left), Kir4.1 currents displayed their characteristic mild inward rectification. In the presence of quinacrine (Fig. 1A and B, right) outward currents were almost completely reduced, whereas some inward currents were still observed. In fact, at negative voltages to E_K , a slow recovery from block was observed during hyperpolarizing pulses, which suggests that quinacrine slowly dissociates from the channels at these voltages. The normalized current-voltage (I-V) relationships for currents measured at the end of the test pulse are shown in Fig. 1C. Quinacrine inhibited Kir4.1 in a concentration- and voltage-dependent manner.

In order to follow the apparent quinacrine dissociation from Kir4.1 channels, a double pulse protocol was used: the cell was first depolarized to $+60$ mV for 2 s followed by a long (20 s) hyperpolarizing pulse to -140 mV. During depolarization, Kir4.1 currents were strongly inhibited by quinacrine (30 μ M) as expected, but the longer hyperpolarizing pulse induced a recovery of the inward currents that in some cells was almost complete (Fig. 1D). However, in other cells the recovery was only partial at 30 μ M and higher concentrations (data not shown). These results demonstrate that quinacrine blocks the channels during depolarization and slowly dissociates from the channels during repolarization.

2.2. Effect of quinacrine on Kir4.1 inside-out patches

Since virtually all of the known Kir4.1 channels blockers have access to the channels from the cytoplasm (polyamines, Mg^{2+} , antidepressants, chloroethylclonidine), we tested the effect of quinacrine in excised inside-out patches, applying the drug directly to the intracellular side of the membrane. To evoke the currents, from a holding potential of -80 mV, a 50 s test pulse to $+80$ mV was applied followed by a 45 s repolarization to -80 mV. In this configuration, the steady-state effect was fast and it was already established at the first recording made at 10 s of the drug perfusion. Fig. 2A–C shows representative Kir4.1 current traces in the absence (control) and presence of 1 (A), 10 (B) and 100 μ M (C) quinacrine. Under control conditions, in absence of Mg^{2+} and polyamines, large outward and inward currents were observed. Application of quinacrine induced a concentration-dependent decrease of outward currents, whereas a slow and complete recovery from block was observed after the membrane potential was returned to -80 mV. These results suggest that quinacrine has access to Kir4.1 channels from the cytoplasm. Fig. 2D shows the concentration-dependent effects of quinacrine on Kir4.1 channels at $+80$ mV, the drug blocked the Kir4.1 outward currents with an IC_{50} of 1.8 ± 0.3 μ M and a Hill coefficient of 0.97 ± 0.1 .

2.3. Blocking and unblocking kinetics of quinacrine on Kir4.1 channels

We next examined the kinetics of block and unblock of quinacrine on Kir4.1 channels from inside-out recordings like those shown in the inset of Fig. 3A. We analyzed the blocking and unblocking kinetics at concentrations 30 and 100 μM . The time courses of the quinacrine effect during the depolarizing and hyperpolarizing steps were obtained by dividing the current recorded in the presence of the drug by the control current ($I_{\text{drug}}/I_{\text{control}}$). These current ratios were fitted to a double and single exponential function to obtain the blocking and unblocking time constants (Fig. 3A). The results are summarized in Fig. 3B and C. The blocking kinetics shows concentration dependence, whereas the unblocking kinetics was not significantly different at 30 and 100 μM , suggesting that quinacrine binds either to a single site in the intracellular face of Kir4.1 channels or to multiple sites with similar unblocking kinetics.

2.4. The quinacrine binding site is within the Kir4.1 central cavity

Previous studies showed that antidepressants like fluoxetine and nortriptyline and the compound chloroethylclonidine block Kir4.1 channels interacting with residues located in the transmembrane pore (Furutani et al., 2009; Rodriguez-Menchaca et al., 2016). Therefore, we performed molecular modeling to define the lowest binding free energy pose for quinacrine within the conduction pathway of Kir4.1 channels. The docking results show that quinacrine interacts with Kir4.1 channels through hydrogen-bonds and hydrophobic contacts (Fig. S2 and Table S1). In the lowest energy pose, the positively charged alkylamino nitrogen (N3) of quinacrine interacts with the glutamic acid side chains at position 158 (Glu158 from subunit A) forming a salt bridge. Additionally, three hydrogen-bonds are formed between quinacrine and Kir4.1 channels. The quinoline ring nitrogen (N5) of quinacrine interacts with the residue Glu158 (subunit B) of Kir4.1, and the residues Thr127 (subunit D) and Thr128 (subunit D) interact with the alkylamino nitrogen (N4) of quinacrine (Fig. S2). The backbone oxygen atom of T127 seems to form the hydrogen-bond with the nitrogen (N4) in the Qn molecule (Fig. S2). From these results, we generated three point mutations on Kir4.1 channels (E158N, T127A and T128A) to test the effect of quinacrine on excised inside-out patches. Fig. 4A–D shows the effect of 10 μM quinacrine on Kir4.1 WT and mutant channels. The patch was held at -80 mV, and a voltage step to $+80$ mV for 50 s was applied followed by a 45 s pulse to -80 mV. In WT channels, 10 μM quinacrine inhibited 88.3 ± 1.5 % of the outward currents. Similar results were obtained with the T127A mutation (89.7 ± 1.1 %), whereas in the mutants T128A (66.1 ± 1.1 %) and E158N (79.8 ± 2.2 %) the inhibition was significantly reduced (Fig. 4E). Additionally, the unblocking of quinacrine in the E158N mutant was clearly accelerated (Fig. 4D), indicating that this residue is very important for the stabilization of quinacrine within the Kir4.1 pore.

Finally, taking into account our experimental data, the 3D binding model of quinacrine within the Kir4.1 channel cavity is shown in Fig. 5. This model depicts the transmembrane domain of the channel, showing only three subunits, A, B, and D.

3. Discussion

Kir4.1 is an inwardly rectifying K⁺ channel highly expressed in glia and kidney. In glial cells, Kir4.1 has been implicated in several functions including extracellular K⁺ homeostasis, maintenance of the resting potential, cell volume regulation, and facilitation of glutamate uptake (Nwaobi et al., 2016). In kidney, Kir4.1 plays a role in K⁺ recycling across the basolateral membrane in corresponding nephron segments and in generating negative membrane potential (Palygin et al., 2016). Therefore, modulating Kir4.1 channels activity would influence the function of these important systems.

In this study, we examined the effect of quinacrine on Kir4.1 channels expressed in HEK293 cells. Quinacrine inhibited Kir4.1 channels in a concentration- and voltage-dependent manner and with extremely slow blocking and unblocking kinetics. Our results indicate that the drug binds to the central cavity of the channel stabilized primarily by a glutamic acid at position 158 with the contribution of the residue T128.

In our whole-cell experiments (Fig. 1), quinacrine strongly inhibited outward and inward Kir4.1 currents. However, the inward currents showed a slow time-dependent recovery as a result of the slow quinacrine dissociation from the channels. Therefore, a long hyperpolarizing pulse was required to fully recover the currents (Fig. 1D). The blocking effect of quinacrine during depolarizations and its dissociation from the channels at voltages negative to E_K mimic the effect of internally applied drugs (e.g., chloroquine, pentamidine, chloroethylclonidine) on Kir channels (Rodríguez-Menchaca et al., 2008; de Boer et al., 2010; Rodríguez-Menchaca et al., 2016). It is therefore conceivable that quinacrine blocks the Kir4.1 channels from the inside after permeating into the cells. Thus, we applied quinacrine to inside-out patches expressing Kir4.1 channels. Under this condition, quinacrine blocked Kir4.1 channels during the depolarizing pulse and completely dissociated from the channels during the repolarization at all concentrations tested (Fig. 2), suggesting that quinacrine acts on Kir4.1 channels from the inside of the plasma membrane. The Hill coefficient for the concentration-response curve of quinacrine in blocking Kir4.1 was close to one (Fig. 2D), suggesting that quinacrine blocks Kir4.1 channels through a 1:1 interaction. This is also supported by the fact that the time constants for unblock at 30 and 100 μM of quinacrine were similar (Fig. 3C).

Virtually all of the reported blockers of Kir4.1 bind to residues of the central cavity of the channel (Furutani et al., 2009; Rodríguez-Menchaca et al., 2016). In this work, we performed molecular modeling followed by mutagenesis studies to identify the site of interaction of quinacrine. Similar to antidepressants and chloroethylclonidine (Furutani et al., 2009; Rodríguez-Menchaca et al., 2016), quinacrine appears to interact with residues of the central cavity of Kir4.1. The positively charged alkylamino nitrogen of quinacrine forms a salt bridge with the glutamic acid side chains at position 158 (E158). Additionally, three hydrogen-bonds are formed between quinacrine and Kir4.1 (Fig. S2 and Table S1). Furthermore, E158 seems to be responsible for the slow unblocking kinetics of quinacrine from Kir4.1 channels (Fig. 3C) since its neutralization accelerated this process (Fig. 4D). These results suggest that E158 is the most important residue for quinacrine interaction, yet the mutant T128A had the biggest effect on quinacrine block.

Contrary to quinacrine, we previously showed that chloroethylclonidine blocks Kir4.1 channels with very fast kinetics (Rodríguez-Menchaca et al., 2016). Although these drugs are positively charged at physiological pH and both interact with residues of the central cavity of the channel (T128 and E158), quinacrine is a bulkier molecule compared to chloroethylclonidine (Fig. S3). This could explain the differences in the blocking and unblocking kinetics between these drugs.

It has been reported that quinacrine inhibits Kir2.x and Kir6.2 channels by a fast-onset pore-block and also by a slow-onset PIP₂-interference mechanisms (Lopez-Izquierdo et al., 2011). Here, given the extremely slow kinetics of quinacrine unblock on Kir4.1 channels ($\tau \sim 9$ s), we cannot rule out the possibility that quinacrine disrupts the PIP₂-Kir4.1 channel interaction. Even though, since Kir4.1 channels have the strongest affinity for PIP₂ out of all the Kir channels (Du et al., 2004), it would be expected that Kir4.1 currents are less inhibited by PIP₂-sequestering drugs.

There are many potential consequences if Kir4.1 is absent or dysfunctional within the brain (Djukic et al., 2007; Kucheryavykh et al., 2007; Haj-Yasein et al., 2011). It has been suggested that dysfunction of Kir4.1 channels disrupt spatial K⁺ buffering by astrocytes, elevates extracellular levels of K⁺ and glutamate and causes abnormal excitation of neurons, leading to an increased seizure activity (Djukic et al., 2007; Kucheryavykh et al., 2007). In this context, the inhibition of Kir4.1 by pore blocking drugs could also induce these abnormalities.

Quinacrine is able to accumulate in mice brains at concentrations nearly 1 μ M (Ghaemmaghami et al., 2009). This value represents the quinacrine concentration in a brain homogenate. However, the intracellular concentration of quinacrine is typically 30 to 50 times higher than its extracellular concentration (Gayraud et al., 2005). The IC₅₀ for inhibition of Kir4.1 channels by quinacrine was 1.8 ± 0.3 μ M (Fig. 4D), a concentration lightly above the brain concentrations reported in animal models (Huang et al., 2006; Ghaemmaghami et al., 2009). Some side effects of quinacrine have been reported affecting the central nervous system, including restlessness, vertigo, insomnia, nightmares, hyperirritability, psychosis, and seizures (Borda and Krant, 1967; Jaeger et al., 1987; Nash et al., 2001, Ehsanian et al, 2011). Particularly, seizures could be related to its effect on Kir4.1 channels. Even though, further studies are required to elucidate the relation between Kir4.1 blockade and the development of seizures.

4. Conclusion

This study demonstrated that quinacrine causes a concentration- and voltage dependent block of Kir4.1 by interacting with residues of the central cavity of the channel. Although is unclear at present, the blockade of Kir4.1 channels could have significant clinical consequences.

5. Experimental procedure

5.1. Molecular Biology and Cell Transfection

The cDNA encoding the rat Kir4.1 subunit (kind gift from C. G. Nichols, Washington University, St. Louis, MO, USA) was subcloned into the mammalian expression vector pcDNA3.1 (Invitrogen, Carlsbad, CA, USA). Mutations were made using the QuikChange Site-Directed Mutagenesis kit (Stratagene, La Jolla, CA, USA). All mutations were confirmed by direct DNA sequencing. HEK293 cells were transiently transfected with WT and mutant Kir4.1 plasmids using Lipofectamine 2000 reagent (Invitrogen) according to manufacturer's instructions. A total of 5 µg cDNA was transfected for inside-out and 10 ng for whole-cell experiments.

5.2. Current recordings in HEK293 cells

Macroscopic currents were recorded in the whole-cell and inside-out configurations of the patch clamp technique by using an Axopatch 200B amplifier (Molecular Devices, Sunnyvale, CA, USA). Data acquisition and command potentials were controlled by the pClamp 9.0 software (Molecular Devices). Patch pipettes with a resistance of 1 to 2 MΩ were made from borosilicate capillary glass (World Precision Instruments, Sarasota, FL, USA). Currents were filtered with a four-pole Bessel filter at 1 kHz and digitized at 5 kHz. An agar-KCl bridge was used to ground the bath.

For whole-cell recordings, pipettes were filled with the internal solution that contained (in mM): 110 KCl, 10 HEPES, 5 K₄BAPTA, 5 K₂ATP and 1 MgCl₂; pH 7.2. The bath solution contained (in mM): 104 NaCl, 30 KCl, 1.8 CaCl₂, 1 MgCl₂, 10 HEPES and 10 glucose; pH 7.4. The currents are represented as the current sensitive to block by 10 mM BaCl₂. Inside-out patches were recorded by using a Mg²⁺- and polyamine-free solution on both sides of the patch containing the following: 123 mM KCl, 5 mM K₂EDTA, 7.2 mM K₂HPO₄ and 8 mM KH₂PO₄, pH 7.2. To prevent current rundown, K⁺-fluoride, K⁺-vanadate and K⁺-pyrophosphate were added (Huang et al., 1998). The pH 5.0 condition was sufficient to abolish any detectable current through Kir channels, and off-line subtraction of the pH 5.0 currents was used to subtract endogenous and leak currents prior analysis to avoid an underestimation of the quinacrine potency. All the current traces shown in the paper were corrected for endogenous and leak currents (Fig. S1). In all cases the endogenous/leak currents were less than 3% of the total current.

5.3. Drugs

Quinacrine (Sigma-Aldrich, St. Louis, MO, USA) was dissolved directly in the solutions at the desired concentration. HEK-293 cells were exposed to quinacrine solutions until the steady-state effects were obtained, using a Fast-Step Perfusion System (VC-77SP Warner Instruments, Hamden, CT, USA).

5.4. Molecular modeling and ligand docking

Homology models of Kir4.1 channel were built based on a crystal structure of Kir2.2 channel (PDBID: 3SPI) template. Sequence alignment between Kir4.1 and Kir2.2 channels was generated by ClustalW server (<http://www.genome.jp/tools/clustalw/>). The

MODELLER program (Sali and Blundell, 1993) was used to generate ten initial Kir4.1 channel homology models based on the Kir2.2 structure template, and the one with the best internal DOPE score of the program was selected for predicting quinacrine and the channel interactions.

An automatic molecular docking program, AUTODOCK4.2 (Morris et al., 1998), was used for the docking of quinacrine into the structure of Kir4.1 channel. The AutoDockTools (ADT) was used for the docking simulation setup. The partial atomic charges for quinacrine were calculated using the Gasteiger-Marsili method (Gasteiger and Marsili, 1980). The grid potential maps were generated for the Kir4.1 channel using CHNOCl (i.e., carbon, hydrogen, nitrogen, oxygen and chloride) elements sampled on a uniform grid containing $100 \times 100 \times 100$ points, 0.375 Å apart. The center of the grid box was set to a cluster of residues, E158 and T128 of the channel. The Lamarckian Genetic Algorithm (LGA) was selected to identify the binding conformations of the ligand. Twenty docking simulations were performed and the final docked quinacrine configuration was selected on the basis of docked binding energies.

The predicted quinacrine-Kir4.1 channel complex was further optimized by SYBYL program using a distance-dependent dielectric constant of 5 to simulate the solvation effect in protein environment (Mehler and Solmajer, 1991). The detailed quinacrine-Kir4.1 channel interactions were analyzed by using LIGPLOT program (Wallace et al., 1995).

5.5. Data Analysis

Patch-clamp data were processed by using Clampfit 9.0 (Molecular Devices) and then analyzed in Origin 7 (OriginLab Corp., Northampton, MA, USA). Data are presented as mean \pm SEM. (n = number of cells or patches).

The fractional block of current (f) was plotted as a function of drug concentration ($[D]$), and the data were fitted with a Hill equation: $f = 1 / \{ 1 + (IC_{50}) / [D]^{nh} \}$, to determine the IC_{50} and the Hill coefficient, nh . Statistical significance was evaluated by Student's t test or ANOVA followed by Dunnett's test. Differences were considered significant at $p < 0.05$.

Supplementary Material

Refer to Web version on PubMed Central for supplementary material.

Acknowledgments

The authors wish to thank Miguel Ángel Flores Virgen (Centro Universitario de Investigaciones Biomédicas, Universidad de Colima, Colima, México) for the technical assistance. This work was supported by SEP-CONACYT (México) [Grants CB-2013-01-220546 to J.A.S.-C., CB-2010-01-153394 to T.F and CB-2010-01-157245 to A.A.R.-M.]. The computations were supported by the Center for High Performance Computing at Virginia Commonwealth University, and by National Institutes of Health shared instrumentation grant S10RR027411 to M.C.

References

Bockenbauer D, Feather S, Stanescu HC, Bandulik S, Zdebik AA, Reichold M, Tobin J, Lieberer E, Sterner C, Landouere G, Arora R, Sirimanna T, Thompson D, Cross JH, van't Hoff W, Al Masri O,

- Tullus K, Yeung S, Anikster Y, Klootwijk E, Hubank M, Dillon MJ, Heitzmann D, Arcos-Burgos M, Knepper MA, Dobbie A, Gahl WA, Warth R, Sheridan E, Kleta R. Epilepsy, ataxia, sensorineural deafness, tubulopathy, and KCNJ10 mutations. *N Engl J Med*. 2009 May 7; 360(19): 1960–70. DOI: 10.1056/NEJMoa0810276 [PubMed: 19420365]
- Borda I, Krant M. Convulsions following intrapleural administration of quinacrine hydrochloride. *JAMA*. 1967 Sep 25; 201(13):1049–50. [PubMed: 6072485]
- Buono RJ, Lohoff FW, Sander T, Sperling MR, O'Connor MJ, Dlugos DJ, Ryan SG, Golden GT, Zhao H, Scattergood TM, Berrettini WH, Ferraro TN. Association between variation in the human KCNJ10 potassium ion channel gene and seizure susceptibility. *Epilepsy Res*. 2004 Feb; 58(2–3): 175–83. [PubMed: 15120748]
- Dai AI, Akcali A, Koska S, Oztuzcu S, Cengiz B, Demiryürek AT. Contribution of KCNJ10 gene polymorphisms in childhood epilepsy. *J Child Neurol*. 2015 Mar; 30(3):296–300. DOI: 10.1177/0883073814539560 [PubMed: 25008907]
- Das S, Tripathi N, Preet R, Siddharth S, Nayak A, Bharatam PV, Kundu CN. Quinacrine induces apoptosis in cancer cells by forming a functional bridge between TRAIL-DR5 complex and modulating the mitochondrial intrinsic cascade. *Oncotarget*. 2016 Aug 17. doi: 10.18632/oncotarget.11335
- de Boer TP, Nalos L, Sary A, Kok B, Houtman MJ, Antoons G, van Veen TA, Beekman JD, de Groot BL, Opthof T, Rook MB, Vos MA, van der Heyden MA. The anti-protozoal drug pentamidine blocks KIR2.x-mediated inward rectifier current by entering the cytoplasmic pore region of the channel. *Br J Pharmacol*. 2010 Apr; 159(7):1532–41. DOI: 10.1111/j.1476-5381.2010.00658.x [PubMed: 20180941]
- Djukic B, Casper KB, Philpot BD, Chin LS, McCarthy KD. Conditional knock out of Kir4.1 leads to glial membrane depolarization, inhibition of potassium and glutamate uptake, and enhanced short-term synaptic potentiation. *J Neurosci*. 2007 Oct 17; 27(42):11354–65. [PubMed: 17942730]
- Eriksson A, Österroos A, Hassan S, Gullbo J, Rickardson L, Jarvius M, Nygren P, Fryknäs M, Höglund M, Larsson R. Drug screen in patient cells suggests quinacrine to be repositioned for treatment of acute myeloid leukemia. *Blood Cancer J*. 2015 Apr 17.5:e307. doi: 10.1038/bcj.2015.31 [PubMed: 25885427]
- Ehsanian R, Van Waes C, Feller SM. Beyond DNA binding - a review of the potential mechanisms mediating quinacrine's therapeutic activities in parasitic infections, inflammation, and cancers. *Cell Commun Signal*. 2011 May 15.9:13. doi: 10.1186/1478-811X-9-13 [PubMed: 21569639]
- Ferraro TN, Golden GT, Smith GG, Martin JF, Lohoff FW, Gieringer TA, Zamboni D, Schwebel CL, Press DM, Kratzer SO, Zhao H, Berrettini WH, Buono RJ. Fine mapping of a seizure susceptibility locus on mouse Chromosome 1: nomination of Kcnj10 as a causative gene. *Mamm Genome*. 2004 Apr; 15(4):239–51. [PubMed: 15112102]
- Furutani K, Ohno Y, Inanobe A, Hibino H, Kurachi Y. Mutational and in silico analyses for antidepressant block of astroglial inward-rectifier Kir4.1 channel. *Mol Pharmacol*. 2009 Jun; 75(6):1287–95. DOI: 10.1124/mol.108.052936 [PubMed: 19264848]
- Gasteiger J, Marsili M. Iterative partial equalization of orbital electronegativity: a rapid access to atomic charges. *Tetrahedron*. 1980; 36(22):3219–3228.
- Gayraud V, Picard-Hagen N, Viguié C, Laroute V, Andréoletti O, Toutain PL. A possible pharmacological explanation for quinacrine failure to treat prion diseases: pharmacokinetic investigations in a ovine model of scrapie. *Br J Pharmacol*. 2005 Feb; 144(3):386–93. [PubMed: 15655516]
- Ghaemmaghami S, Ahn M, Lessard P, Giles K, Legname G, DeArmond SJ, Prusiner SB. Continuous quinacrine treatment results in the formation of drug-resistant prions. *PLoS Pathog*. 2009 Nov. 5(11):e1000673. doi: 10.1371/journal.ppat.1000673 [PubMed: 19956709]
- Gilliam D, O'Brien DP, Coates JR, Johnson GS, Johnson GC, Mhlanga-Mutangadura T, Hansen L, Taylor JF, Schnabel RD. A homozygous KCNJ10 mutation in Jack Russell Terriers and related breeds with spinocerebellar ataxia with myokymia, seizures, or both. *J Vet Intern Med*. 2014 May-Jun; 28(3):871–7. DOI: 10.1111/jvim.12355 [PubMed: 24708069]
- Haj-Yasein NN, Jensen V, Vindedal GF, Gundersen GA, Klungland A, Ottersen OP, Hvalby O, Nagelhus EA. Evidence that compromised K⁺ spatial buffering contributes to the epileptogenic

- effect of mutations in the human Kir4.1 gene (KCNJ10). *Glia*. 2011 Nov; 59(11):1635–42. DOI: 10.1002/glia.21205 [PubMed: 21748805]
- Hibino H, Inanobe A, Furutani K, Murakami S, Findlay I, Kurachi Y. Inwardly rectifying potassium channels: their structure, function, and physiological roles. *Physiol Rev*. 2010 Jan; 90(1):291–366. DOI: 10.1152/physrev.00021.2009 [PubMed: 20086079]
- Huang CL, Feng S, Hilgemann DW. Direct activation of inward rectifier potassium channels by PIP2 and its stabilization by Gbetagamma. *Nature*. 1998 Feb 19; 391(6669):803–6. [PubMed: 9486652]
- Huang Y, Okochi H, May BC, Legname G, Prusiner SB, Benet LZ, Guglielmo BJ, Lin ET. Quinacrine is mainly metabolized to mono-desethyl quinacrine by CYP3A4/5 and its brain accumulation is limited by P-glycoprotein. *Drug Metab Dispos*. 2006 Jul; 34(7):1136–44. [PubMed: 16581945]
- Jaeger A, Sauder P, Kopferschmitt J, Flesch F. Clinical features and management of poisoning due to antimalarial drugs. *Med Toxicol Adverse Drug Exp*. 1987 Jul-Aug; 2(4):242–73. [PubMed: 3306266]
- Khurana A, Roy D, Kalogera E, Mondal S, Wen X, He X, Dowdy S, Shridhar V. Quinacrine promotes autophagic cell death and chemosensitivity in ovarian cancer and attenuates tumor growth. *Oncotarget*. 2015 Nov 3; 6(34):36354–69. DOI: 10.18632/oncotarget.5632 [PubMed: 26497553]
- Kucheryavykh YV, Kucheryavykh LY, Nichols CG, Maldonado HM, Baksi K, Reichenbach A, Skatchkov SN, Eaton MJ. Downregulation of Kir4.1 inward rectifying potassium channel subunits by RNAi impairs potassium transfer and glutamate uptake by cultured cortical astrocytes. *Glia*. 2007 Feb; 55(3):274–81. [PubMed: 17091490]
- Lachheb S, Cluzeaud F, Bens M, Genete M, Hibino H, Lourdel S, Kurachi Y, Vandewalle A, Teulon J, Paulais M. Kir4.1/Kir5.1 channel forms the major K⁺ channel in the basolateral membrane of mouse renal collecting duct principal cells. *Am J Physiol Renal Physiol*. 2008 Jun; 294(6):F1398–407. DOI: 10.1152/ajprenal.00288.2007 [PubMed: 18367659]
- Lenzen KP, Heils A, Lorenz S, Hempelmann A, Höfels S, Lohoff FW, Schmitz B, Sander T. Supportive evidence for an allelic association of the human KCNJ10 potassium channel gene with idiopathic generalized epilepsy. *Epilepsy Res*. 2005 Feb; 63(2–3):113–8. [PubMed: 15725393]
- López-Izquierdo A, Aréchiga-Figueroa IA, Moreno-Galindo EG, Ponce-Balbuena D, Rodríguez-Martínez M, Ferrer-Villada T, Rodríguez-Menchaca AA, van der Heyden M, Sánchez-Chapula JA. Mechanisms for Kir channel inhibition by quinacrine: acute pore block of Kir2. x channels and interference in PIP2 interaction with Kir2. x and Kir6. 2 channels. *Pflugers Arch - Eur J Physiol*. 2011 Jul; 462(4):505–517. [PubMed: 21779761]
- Loudon KW, Fry AC. The renal channelopathies. *Ann Clin Biochem*. 2014 Jul; 51(Pt 4):441–58. DOI: 10.1177/0004563214531403 [PubMed: 24662008]
- Lourdel S, Paulais M, Cluzeaud F, Bens M, Tanemoto M, Kurachi Y, Vandewalle A, Teulon J. An inward rectifier K(+) channel at the basolateral membrane of the mouse distal convoluted tubule: similarities with Kir4-Kir5.1 heteromeric channels. *J Physiol*. 2002 Jan 15; 538(Pt 2):391–404. [PubMed: 11790808]
- Mehler EL, Solmajer T. Electrostatic effects in proteins: comparison of dielectric and charge models. *Protein Eng*. 1991 Dec; 4(8):903–10. [PubMed: 1667878]
- Morris GM, Goodsell DS, Halliday LS, Huey R, Hart WE, Belew RK, Olson AJ. Automated docking using a Lamarckian genetic algorithm and an empirical binding free energy function. *J Comput Chem*. 1998 Nov 15; 19(14):1639–1662.
- Nash TE, Ohl CA, Thomas E, Subramanian G, Keiser P, Moore TA. Treatment of patients with refractory giardiasis. *Clin Infect Dis*. 2001 Jul 1; 33(1):22–8. [PubMed: 11389490]
- Neusch C, Papadopoulos N, Müller M, Maletzki I, Winter SM, Hirrlinger J, Handschuh M, Bähr M, Richter DW, Kirchhoff F, Hülsmann S. Lack of the Kir4.1 channel subunit abolishes K⁺ buffering properties of astrocytes in the ventral respiratory group: impact on extracellular K⁺ regulation. *J Neurophysiol*. 2006 Mar; 95(3):1843–52. [PubMed: 16306174]
- Neznanov N, Gorbachev AV, Neznanova L, Komarov AP, Gurova KV, Gasparian AV, Banerjee AK, Almasan A, Fairchild RL, Gudkov AV. Anti-malaria drug blocks proteotoxic stress response: anti-cancer implications. *Cell Cycle*. 2009 Dec; 8(23):3960–70. [PubMed: 19901558]

- Nwaobi SE, Cuddapah VA, Patterson KC, Randolph AC, Olsen ML. The role of glial-specific Kir4.1 in normal and pathological states of the CNS. *Acta Neuropathol.* 2016 Jul; 132(1):1–21. DOI: 10.1007/s00401-016-1553-1 [PubMed: 26961251]
- Ohno Y, Hibino H, Lossin C, Inanobe A, Kurachi Y. Inhibition of astroglial Kir4.1 channels by selective serotonin reuptake inhibitors. *Brain Res.* 2007 Oct 31; 1178:44–51. [PubMed: 17920044]
- Palygin O, Pochynyuk O, Staruschenko A. Role and mechanisms of regulation of the basolateral K(ir) 4.1/K(ir) 5.1 K(+) channels in the distal tubules. *Acta Physiol (Oxf).* 2016 Apr 30. doi: 10.1111/apha.12703
- Preet R, Mohapatra P, Mohanty S, Sahu SK, Choudhuri T, Wyatt MD, Kundu CN. Quinacrine has anticancer activity in breast cancer cells through inhibition of topoisomerase activity. *Int J Cancer.* 2012 Apr 1; 130(7):1660–70. DOI: 10.1002/ijc.26158 [PubMed: 21544805]
- Reichold M, Zdebik AA, Lieberer E, Rapedius M, Schmidt K, Bandulik S, Sterner C, Tegtmeier I, Penton D, Baukowitz T, Hulton SA, Witzgall R, Ben-Zeev B, Howie AJ, Kleta R, Bockenhauer D, Warth R. KCNJ10 gene mutations causing EAST syndrome (epilepsy, ataxia, sensorineural deafness, and tubulopathy) disrupt channel function. *Proc Natl Acad Sci U S A.* 2010 Aug 10; 107(32):14490–5. DOI: 10.1073/pnas.1003072107 [PubMed: 20651251]
- Rodríguez-Menchaca AA, Aréchiga-Figueroa IA, Sánchez-Chapula JA. The molecular basis of chloroethylclonidine block of inward rectifier (Kir2.1 and Kir4.1) K(+) channels. *Pharmacol Rep.* 2016 Apr; 68(2):383–9. DOI: 10.1016/j.pharep.2015.10.005 [PubMed: 26922543]
- Rodríguez-Menchaca AA, Navarro-Polanco RA, Ferrer-Villada T, Rupp J, Sachse FB, Tristani-Firouzi M, Sánchez-Chapula JA. The molecular basis of chloroquine block of the inward rectifier Kir2.1 channel. *Proc Natl Acad Sci U S A.* 2008 Jan 29; 105(4):1364–8. DOI: 10.1073/pnas.0708153105 [PubMed: 18216262]
- Sali A, Blundell TL. Comparative protein modelling by satisfaction of spatial restraints. *J Mol Biol.* 1993 Dec 5; 234(3):779–815. [PubMed: 8254673]
- Scholl UI, Choi M, Liu T, Ramaekers VT, Häusler MG, Grimmer J, Tobe SW, Farhi A, Nelson-Williams C, Lifton RP. Seizures, sensorineural deafness, ataxia, mental retardation, and electrolyte imbalance (SeSAME syndrome) caused by mutations in KCNJ10. *Proc Natl Acad Sci U S A.* 2009 Apr 7; 106(14):5842–7. DOI: 10.1073/pnas.0901749106 [PubMed: 19289823]
- Sicca F, Imbrici P, D'Adamo MC, Moro F, Bonatti F, Brovedani P, Grottesi A, Guerrini R, Masi G, Santorelli FM, Pessia M. Autism with seizures and intellectual disability: possible causative role of gain-of-function of the inwardly-rectifying K+ channel Kir4.1. *Neurobiol Dis.* 2011 Jul; 43(1): 239–47. DOI: 10.1016/j.nbd.2011.03.016 [PubMed: 21458570]
- Simard M, Nedergaard M. The neurobiology of glia in the context of water and ion homeostasis. *Neuroscience.* 2004; 129(4):877–96. [PubMed: 15561405]
- Su S, Ohno Y, Lossin C, Hibino H, Inanobe A, Kurachi Y. Inhibition of astroglial inwardly rectifying Kir4.1 channels by a tricyclic antidepressant, nortriptyline. *J Pharmacol Exp Ther.* 2007 Feb; 320(2):573–80. [PubMed: 17071817]
- Swale DR, Kharade SV, Denton JS. Cardiac and renal inward rectifier potassium channel pharmacology: emerging tools for integrative physiology and therapeutics. *Curr Opin Pharmacol.* 2014 Apr. 15:7–15. [PubMed: 24721648]
- Tong X, Ao Y, Faas GC, Nwaobi SE, Xu J, Hausteine MD, Anderson MA, Mody I, Olsen ML, Sofroniew MV, Khakh BS. Astrocyte Kir4.1 ion channel deficits contribute to neuronal dysfunction in Huntington's disease model mice. *Nat Neurosci.* 2014 May; 17(5):694–703. DOI: 10.1038/nn.3691 [PubMed: 24686787]
- Wallace AC, Laskowski RA, Thornton JM. LIGPLOT: a program to generate schematic diagrams of protein-ligand interactions. *Protein Eng.* 1995 Feb; 8(2):127–34. [PubMed: 7630882]
- Wilcock DM, Vitek MP, Colton CA. Vascular amyloid alters astrocytic water and potassium channels in mouse models and humans with Alzheimer's disease. *Neuroscience.* 2009 Mar 31; 159(3): 1055–69. DOI: 10.1016/j.neuroscience.2009.01.023 [PubMed: 19356689]
- Zhang Y, Xu G, Ling Q, Da C. Expression of aquaporin 4 and Kir4.1 in diabetic rat retina: treatment with minocycline. *J Int Med Res.* 2011; 39(2):464–79. [PubMed: 21672350]
- Zhao M, Bousquet E, Valamanesh F, Farman N, Jeanny JC, Jaisser F, Behar-Cohen FF. Differential regulations of AQP4 and Kir4.1 by triamcinolone acetonide and dexamethasone in the healthy and

inflamed retina. Invest Ophthalmol Vis Sci. 2011 Aug 11; 52(9):6340–7. DOI: 10.1167/iovs.11-7675 [PubMed: 21724913]

Author Manuscript

Author Manuscript

Author Manuscript

Author Manuscript

Highlights

- Quinacrine blocks Kir4.1 channels in a concentration and voltage dependent manner
- Quinacrine have access to Kir4.1 channels from the cytoplasm
- Quinacrine blocks Kir4.1 by plugging the central cavity of the channels

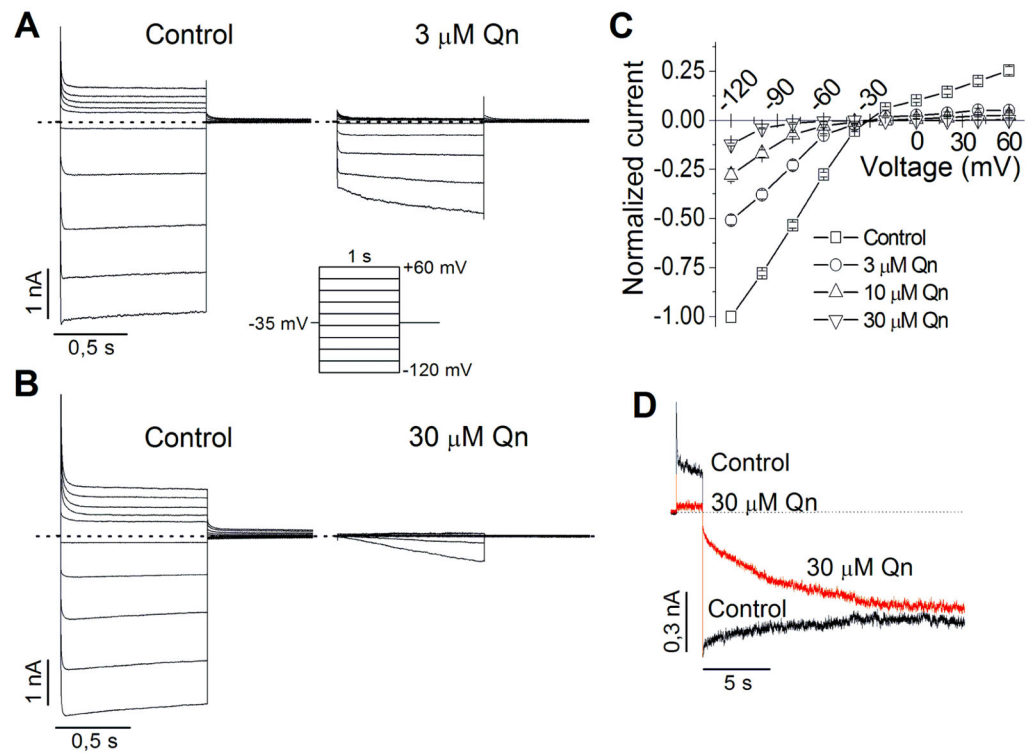


Figure 1.

Effect of quinacrine (Qn) on Kir4.1 channels expressed in HEK293 cells and recorded under whole-cell configuration. (A–B) Representative Kir4.1 current traces in absence (control) and presence of 3 (A) and 30 μM (B) Qn. Here and hereafter, dotted lines define the zero current level. (C) Average steady-state I–V curves in the absence and presence of Qn at the indicated concentrations (n=5). (D) Representative Kir4.1 current traces elicited by a 2 s depolarizing pulse followed by a long (20 s) repolarizing pulse in absence (control) and presence of 30 μM Qn.

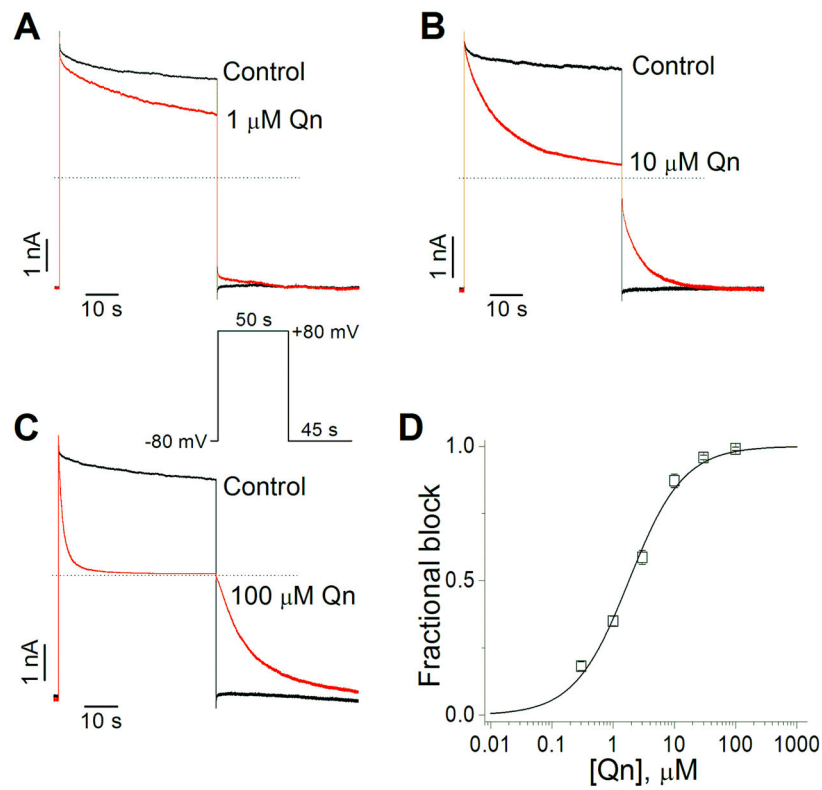


Figure 2. Effect of Qn on Kir4.1 channels expressed in HEK293 cells and recorded in excised inside-out patches. (A–C) Representative Kir4.1 current traces in absence (control) and presence of 1 (A), 10 (B) and 100 μM (C) Qn. (D) Concentration-response curve of the Qn fractional block at +80 mV (n=5–10).

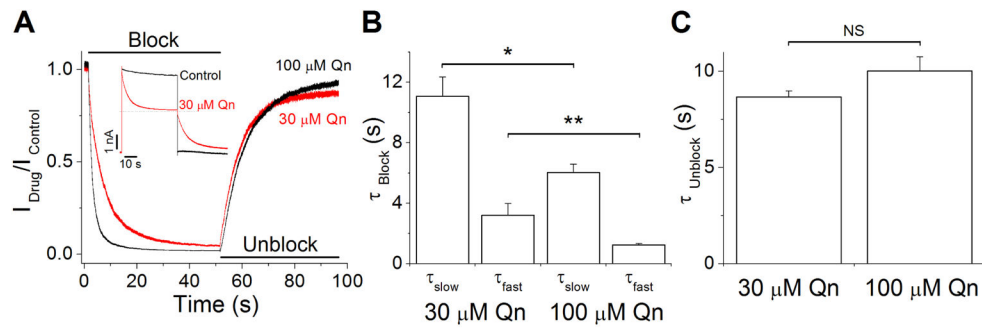


Figure 3.

Blocking and unblocking kinetics of Kir4.1 currents by 30 and 100 μM Qn. (A) Current ratios ($I_{\text{drug}}/I_{\text{control}}$) with 30 (red trace) and 100 μM (black trace) Qn generated from recordings like those shown in the inset. Cells were held at -80 mV and stepped to $+80$ mV followed by a repolarization to -80 mV. (B) Time constants of Qn blockade of Kir4.1 currents. (C) Unblocking time constants of Qn. ($n = 5$) * $p < 0.05$, ** $p < 0.01$.

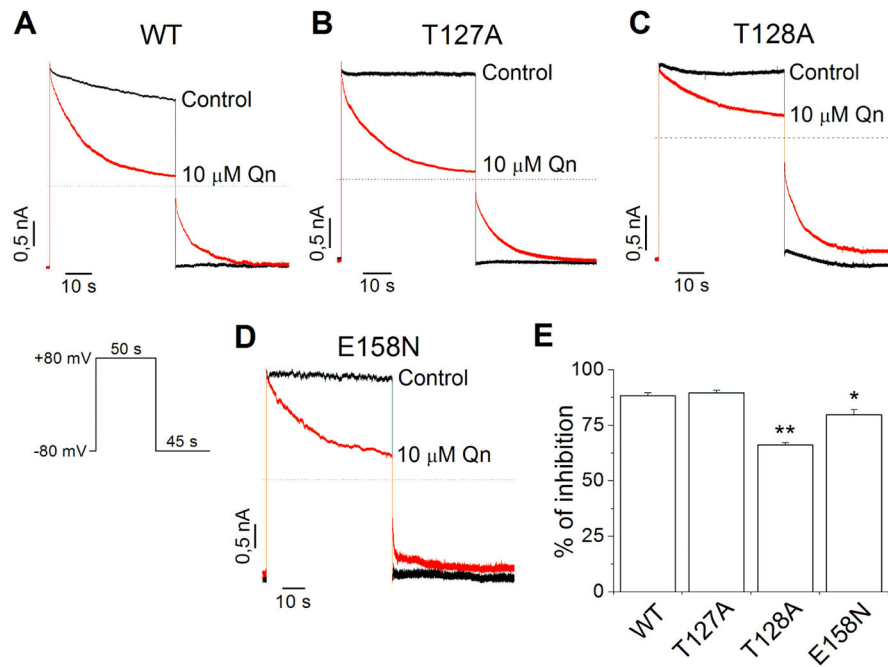


Figure 4.

Qn block is altered by mutations in the central cavity of Kir4.1 channels. Representative Kir4.1WT (A), Kir4.1T127A (B), Kir4.1T128A (C) and Kir4.1E158N (D) current traces in absence (control) and presence of 10 μM Qn. (E) Percentage of inhibition of Kir4.1 currents by 10 μM Qn. (n= 4–6) * $p < 0.05$, ** $p < 0.01$.

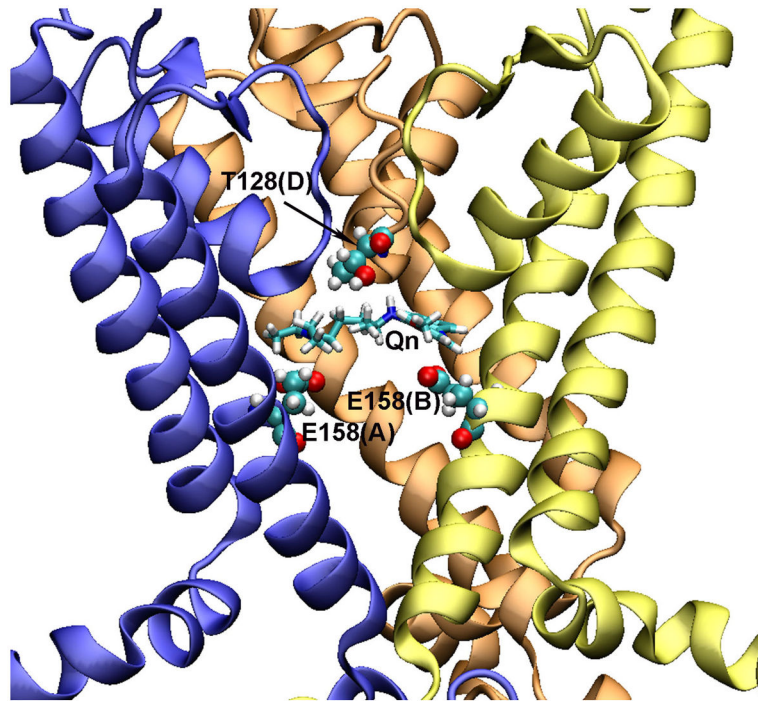


Figure 5. Molecular model of Kir4.1 channel binding pocket with docked Qn. The Kir4.1 channel model is shown in NewCartoon presentation (subunits A, B, and D are in blue, yellow, and orange, respectively. The subunit C was removed for clarity). The Qn is drawn in Licorice, and interacting residues with Qn are drawn in VDW sphere.